

Electronic theory for bilayer effects in high- T_c superconductors

S. Grabowski, J. Schmalian, M. Langer, and K. H. Bennemann

Institut für Theoretische Physik, Freie Universität Berlin, Arnimallee 14, D-14195 Berlin, Germany

(Received 13 August 1996)

The normal and superconducting state of two coupled CuO_2 layers in the high- T_c superconductors are investigated by using the bilayer Hubbard model, the fluctuation exchange approximation on the real frequency axis, and the Eliashberg theory. We find that the planes are antiferromagnetically correlated leading to a strongly enhanced shadow band formation. Furthermore, the interlayer hopping is renormalized which causes a blocking of the interplane charge transfer for low doping. Finally, the superconducting order parameter has a $d_{x^2-y^2}$ symmetry with significant interlayer contributions and a larger *optimal doping* with respect to the single layer. [S0163-1829(97)04805-4]

The importance of the multiple CuO_2 layers within the high- T_c superconductors like $\text{Bi}_2\text{Sr}_2\text{CaCu}_2\text{O}_{8+\delta}$ (BSCCO) or $\text{YBa}_2\text{Cu}_3\text{O}_{6+\delta}$ (YBCO) is intensively studied. Neutron-scattering experiments show evidence that antiferromagnetically correlated spin fluctuations are quite strong between the bilayers in YBCO.¹ Recent angular-resolved photoemission (ARPES) experiments found indications for two separated bands in YBCO,² that might be related to the existence of two CuO_2 bands caused by a interplane quasiparticle transfer. However, the small observed bilayer splitting in YBCO and the difficulty to resolve two bands in BSCCO (Refs. 3 and 4) support the idea that short-ranged antiferromagnetic correlations in the cuprates alter the electronic excitations and reduces the interlayer hopping.

In this Brief Report we study the bilayer Hubbard Hamiltonian within the fluctuation exchange (FLEX) approximation.⁵ We find that the antiferromagnetically correlated planes yield strong deformations of the quasiparticle dispersions and a blocking of the effective interlayer hopping for small doping concentrations and low excitation energies. For YBCO- and BSCCO-like systems we observe that the shadows of the Fermi surface⁶ (FS) occur only when the interplane coupling is considered. The superconducting state has a $d_{x^2-y^2}$ symmetry with inter- and intralayer Cooper pair formation. The *optimal doping* for bilayers, where T_c becomes maximal, shifts to larger doping concentrations compared to a single CuO_2 plane.

Previously, bilayer effects have been studied microscopically by incorporating solely a magnetic coupling⁷ and within the bilayer Hubbard model by including either an interplane hopping⁸⁻¹¹ or an interlayer Coulomb repulsion.¹¹ Furthermore, by assuming $V_\perp = -V_\parallel$ for the intralayer (V_\parallel) and the interlayer (V_\perp) interactions, it has been shown that bilayer correlations might lead to a superconducting s -wave order parameter.^{11,12} This has opposite signs in the two CuO_2 bands (s^\pm state) which corresponds to an interlayer pairing state. However, it is *a priori* not evident that these models which correspond to perfectly correlated bilayers via $V_\perp \equiv -V_\parallel$ apply to real systems like YBCO or BSCCO. Consequently, it is of interest for a further understanding of the high- T_c materials to use a fully self-consistent approach to determine V_\parallel and V_\perp independently.

Our theory is based on the bilayer Hubbard model:

$$H = \sum_{i,j,l,l',\sigma} (t_{j,l'}^{i,l} - \mu \delta_{j,l'}^{i,l}) c_{i,l,\sigma}^\dagger c_{j,l',\sigma} + U \sum_{i,l} n_{i,l,\uparrow} n_{i,l,\downarrow}.$$

Here the hopping integrals $t_{j,l'}^{i,l}$ determine the bare dispersion $\varepsilon_{ll'}^0(\mathbf{k})$ in two-dimensional \mathbf{k} space, i and j (l and l') are the site (layer) indices, $\delta_{j,l'}^{i,l}$ is the Kronecker symbol, U is the local Coulomb repulsion, and μ is the chemical potential. The interaction-free contribution of the Hamiltonian can be diagonalized yielding an antibonding ($-$) and a bonding band ($+$) with bare dispersion $\varepsilon_\pm^0(\mathbf{k})$. Assuming that this symmetry holds also in the full interacting case, one can define corresponding Greens function $G_\pm(\mathbf{k}, i\omega_m)$ with fermionic Matsubara frequencies $\omega_m = (2m+1)\pi T$ and temperature T . They are connected to the self-energy $\Sigma_\pm(\mathbf{k}, i\omega_m)$ via the Dyson equation $G_\pm(\mathbf{k}, i\omega_m) = 1/\{i\omega_m - [\varepsilon_\pm^0(\mathbf{k}) - \mu] - \Sigma_\pm(\mathbf{k}, i\omega_m)\}$. For the FLEX self-energy one obtains

$$\Sigma_\lambda(\mathbf{k}, i\omega_m) = \sum_{k',\lambda'} V_{\lambda,\lambda'}(\mathbf{k}-\mathbf{k}', i\omega_m - i\omega_{m'}) G_{\lambda'}(\mathbf{k}', i\omega_{m'})$$

with $\Sigma_{k'} = (T/N)\Sigma_{\mathbf{k}', m'}$, band index $\lambda = \pm$, and number of \mathbf{k} points N . Due to the symmetry of the bilayer it follows for the intraband interactions that $V_{++}(\mathbf{k}, i\omega_m) = V_{--}(\mathbf{k}, i\omega_m)$ and for the interband contributions that $V_{+-}(\mathbf{k}, i\omega_m) = V_{-+}(\mathbf{k}, i\omega_m)$. $V_{\lambda,\lambda'}(\mathbf{k}, i\omega_m)$ is obtained by calculating the electron-hole bubble $\chi_{\lambda,\lambda'}(\mathbf{k}, i\omega_m) = -\sum_{k'} G_\lambda(\mathbf{k}+\mathbf{k}', i\omega_m + i\omega_{m'}) G_{\lambda'}(\mathbf{k}', i\omega_{m'})$ and by performing the summation of the FLEX diagrams⁵ in the layer representation yielding an inter-, $V_\perp(\mathbf{k}, i\omega_m)$, and an in-plane, $V_\parallel(\mathbf{k}, i\omega_m)$, interaction:

$$V_{+\pm}(\mathbf{k}, i\omega_m) = 1/2[V_\parallel(\mathbf{k}, i\omega_m) \pm V_\perp(\mathbf{k}, i\omega_m)]. \quad (1)$$

Note, our expression for $V_{++}(\mathbf{k}, i\omega_m)$ and $V_{+-}(\mathbf{k}, i\omega_m)$ are similar to the formulas obtained by Ref. 11 when we neglect the interlayer Coulomb repulsion and take the correct double counting of the second-order diagram into account.

This set of coupled equations is solved self-consistently on the real frequency axis.¹³ The FS topology is characterized by

$$\varepsilon_\pm^0(\mathbf{k}) = -\{2t[\cos(k_x) + \cos(k_y)] + 4t'\cos(k_x)\cos(k_y) + 2t''[\cos(2k_x) + \cos(2k_y)] \pm t_\perp\}$$

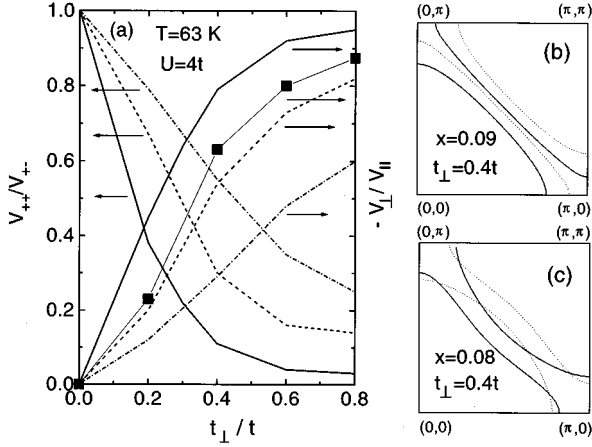


FIG. 1. Dependence of the interactions on the doping and on t_{\perp} . (a) Ratio $-V_{\perp}/V_{\parallel}$ and V_{++}/V_{+-} for the LSCO-like model with $x=0.09$ (solid line), $x=0.12$ (dashed line) and $x=0.16$ (dashed-dotted line) compared with the YBCO model for $x=0.12$ (squares). FS's and their shadows for the LSCO (b) and YBCO-like (c) model.

with intraplane hopping integrals $t=0.25$ eV, $t'=-0.38t$, $t''=-0.06t$,¹⁴ and $t_{\perp}=0.4t=100$ meV (Ref. 15) as the explicit model for YBCO. To investigate the complete dependence of the electronic properties on t_{\perp} we also use a model dispersion with $t'=t''=0$. Since the corresponding FS is similar to the $\text{La}_{2-x}\text{Sr}_x\text{CuO}_4$ system for $t_{\perp}=0$,¹⁶ we call this dispersion for simplicity LSCO-like. However note, LSCO is in distinction to YBCO or BSCCO a monolayer compound and the antiferromagnetic coupling between adjacent planes is weaker across the unit cells. Although the FS of these two in-plane parameter sets differs considerably for $t_{\perp}=0$, they become very similar for finite t_{\perp} as shown in Fig. 1. Consequently, we find that the physical results discussed below do not depend qualitatively on the particular choice of the hopping elements. For comparison with previous results we take $U=4t$ but notice that we find no significant changes in our data up to values of $U=6t$.

In Fig. 1(a) we investigate the interplay between the inter- and intraplane antiferromagnetic correlations upon t_{\perp} and the doping x . For both in-plane dispersion we find that $V_{\parallel}(\mathbf{k}, \omega)$ decreases only slightly when t_{\perp} is increased. Such a behavior was also observed in quantum Monte Carlo (QMC) simulations at half filling.⁹ Since $V_{\perp}(\mathbf{k}, \omega)$ and $V_{\parallel}(\mathbf{k}, \omega)$ have almost same \mathbf{k} dependence, but with opposite signs, the two layers are antiferromagnetically correlated as observed in experiments.¹ As a measure of this phenomenon we plot in Fig. 1(a) the ratio of the corresponding interactions $-V_{\perp}/V_{\parallel} := -V_{\perp}(\mathbf{q}, 0)/V_{\parallel}(\mathbf{q}, 0)$ at their maxima, where $\mathbf{q} \approx \mathbf{Q}$ for the LSCO-like model. Here we observe that the bilayer coupling increases rapidly with increasing t_{\perp} . In addition, it is remarkable that not only $V_{\perp}(\mathbf{k}, \omega)$ and $V_{\parallel}(\mathbf{k}, \omega)$ increase with decreasing doping, but also the ratio $-V_{\perp}/V_{\parallel}$. Thus, the stabilization of the interplane magnetism via a coupling of antiferromagnetically ordered in-plane regions (size $\sim \xi$) across the layers should be most effective for small x . Note, by performing the same analysis in case of the YBCO system we find rather similar results as can be seen in Fig. 1(a) for $x=0.12$ besides that $V_{\parallel}(\mathbf{k}, \omega)$ and $V_{\perp}(\mathbf{k}, \omega)$ are commensurate [$\mathbf{q}=\mathbf{Q}=(\pi, \pi)$],¹⁴ due to the

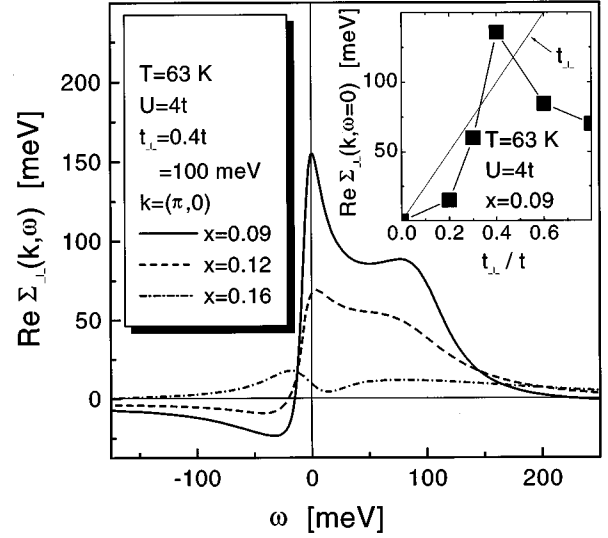


FIG. 2. $\text{Re}\Sigma_{\perp}(\mathbf{k}, \omega)$ for different doping values. Inset: $\text{Re}\Sigma_{\perp}(\mathbf{k}, 0)$ at the FS of the antibonding band versus t_{\perp} .

overdamped nature of the spin excitations. By transforming these results to the band representation via Eq. (1), one sees in Fig. 1(a), where we plot $V_{++}/V_{+-} := V_{++}(\mathbf{q}, 0)/V_{+-}(\mathbf{q}, 0)$, that the contribution of the intraband interactions vanishes rapidly for low doping with t_{\perp} thereby explaining the absence of these excitations in experiments.¹

By investigating the two bands of the LSCO model with $t_{\perp}=0.4t$, we observe similar to Ref. 10 that the bilayer splitting is strongly renormalized from the uncorrelated $\Delta\varepsilon(\mathbf{k}=(\pi, 0))=2t_{\perp}=200$ meV to $\Delta\varepsilon(\mathbf{k}=(\pi, 0))=125$ meV in the case of $x=0.12$.¹⁷ To study the origin of this effect and more interestingly to investigate the low-energy interplane electron dynamics $\text{Re}\Sigma_{\perp}(\mathbf{k}, \omega)=1/2\text{Re}[\Sigma_{+}(\mathbf{k}, \omega)-\Sigma_{-}(\mathbf{k}, \omega)]$ is plotted in Fig. 2 for $\mathbf{k}=(\pi, 0)$ upon doping. This quantity renormalizes t_{\perp} and yields an effective frequency and momentum-dependent interplane hopping amplitude $\tilde{t}_{\perp}(\mathbf{k}, \omega)=t_{\perp}-\text{Re}\Sigma_{\perp}(\mathbf{k}, \omega)$, which follows directly from the matrix Dyson equation in the layer representation. The sign of $\text{Re}\Sigma_{\perp}(\mathbf{k}, \omega)$ is determined for small ω by the sign of $V_{\perp}(\mathbf{k}, \omega)$, such that we find $\tilde{t}_{\perp}(\mathbf{k}, \omega) \ll t_{\perp}$ for $\omega < t_{\perp}$ and low x ($x < 0.12$). This interesting phenomenon can be found along the entire FS although it is most pronounced at $(\pi, 0)$ and exists for a wide range of t_{\perp} as can be observed in the inset of Fig. 2. Consequently, the effective interplane hopping at the Fermi energy is blocked, which leads to the disappearance of a coherent quasiparticle tunneling process, although, due to the frequency dependence of $\text{Re}\Sigma_{\perp}(\mathbf{k}, \omega)$, both bands are still splitted. Physically, this is related to the fact that each interlayer hopping process is accompanied by spin flips due to the opposite antiferromagnetic environment in the other plane. Thus, due to the corresponding large $\text{Im}\Sigma_{\perp}(\mathbf{k}, \omega)$ an incoherent coupling of the layers occur. The blocking of the c -axis hopping is rather similar to the interesting confinement idea of Ref. 18, although we find that it only occurs for small x . Thus this remarkable doping dependence should be particular important for normal-state c -axis transport properties. Here the experimental observation that *underdoped* LSCO and YBCO systems are charac-

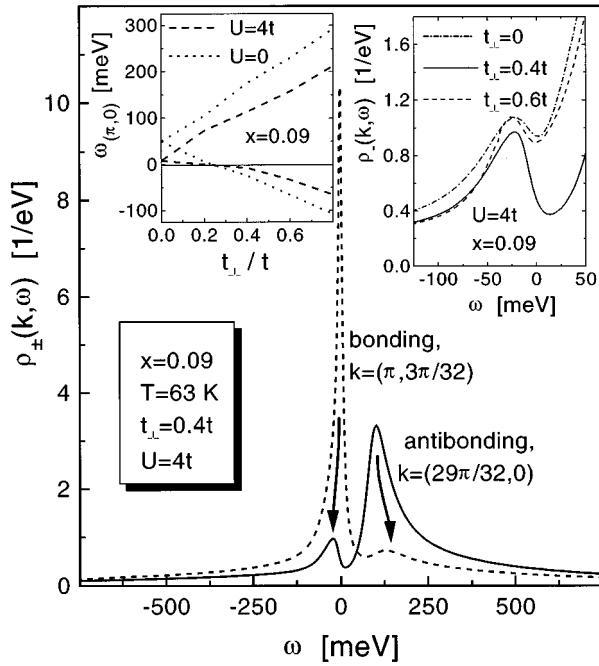


FIG. 3. Spectral density $\rho_{\pm}(\mathbf{k}_{\text{FS}}, \omega)$ for the LSCO-like model. Right inset: Dependence of the shadow state intensity on t_{\perp} . Left inset: Position of the bands at the $(\pi, 0)$ point with respect to the Fermi energy for $U=0$ and $U=4t$.

terized by a semiconductorlike temperature dependence of the resistivity, while *overdoped* cuprates show a metalliclike behavior,¹⁹ might be related to a crossover from a coherent, hoppinglike dynamics to a phonon or impurity-dominated one.²⁰

In Fig. 3 we demonstrate the influence of the interplane coupling on the formation of shadow states in the case of the LSCO-like model. In Ref. 21 we showed that the dynamical antiferromagnetic short-range order in the cuprates leads to a transfer of spectral weight from the FS at \mathbf{k} to its shadow at $\mathbf{k}+\mathbf{Q}$. Now, since we find for a bilayer system that $V_{++}(\mathbf{k}, \omega)$ is small compared to $V_{+-}(\mathbf{k}, \omega)$ for intermediate t_{\perp} , we expect that the spectral weight is not only shifted by the momentum \mathbf{Q} , but simultaneously also from the bonding to the antibonding band and vice versa. This phenomenon is demonstrated in Fig. 3, where we present our results for the spectral density for the bonding ($\rho_{+}(\mathbf{k}_{\text{FS}}, \omega)$) and the antibonding ($\rho_{-}(\mathbf{k}_{\text{FS}}+\mathbf{Q}, \omega)$) band and FS momentum \mathbf{k}_{FS} . There is a transfer from the bonding to the antibonding band leading to an occupied shadow state and in addition a transfer in the reversed direction above the Fermi energy. Most interestingly, the intensity of the shadow states is strongly dependent on the magnitude of the interplane hopping as can be observed in the right inset of Fig. 3. Here the shadow peak is most pronounced for $t_{\perp}=0.4t$ before it decreases again for even larger values of t_{\perp} . To verify that this result is related to an enhanced antiferromagnetic coupling, we investigated $\text{Im}\Sigma_{-}(\mathbf{k}_{\text{FS}}+\mathbf{Q}, 0)$ as a measure of the coupling of the FS to its shadow²¹ and found a corresponding maximum at $t_{\perp}=0.4t$. Therefore, the strongly enhanced formation of shadow states in bilayers is caused by electronic correlations and is related to the already discussed suppression of the bilayer splitting and a corresponding large spectral density at

the Fermi level. This is demonstrated in the left inset of Fig. 3, where we plot the t_{\perp} dependence of the position ($\omega_{(\pi, 0)}$) of the flat quasiparticle band at $(\pi, 0)$ with respect to the Fermi level for $U \neq 0$ and $U=0$. It can be seen that the antibonding band moves away from the Fermi energy ($\omega=0$) ($\sim t_{\perp}$), while the bonding band is tightly pinned at $\omega=0$ up to $t_{\perp} \approx 0.45t$. Note that the shadow state intensity is also enhanced for larger x and most importantly that in a bilayer shadow states can be found up to doping concentrations of $x \approx 0.17$, while they vanish for $x \approx 0.13$ in a single layer compound.

By performing calculations for the YBCO dispersion we find no shadow states for $t_{\perp}=0$ down to $x=0.05$. Therefore, due to the similarity of the YBCO and BSCCO FS's (Ref. 4) the observation by Aebi *et al.*⁶ cannot be satisfactorily understood by considering only a single CuO_2 plane. However, by taking a finite t_{\perp} into account we find for YBCO and BSCCO-like²² systems, in agreement with our results for the LSCO-like model, that the antiferromagnetic coupling increases and that shadow states start to appear for $x < 0.12$ with a maximum intensity at $t_{\perp} \approx 0.4t$. Furthermore the most favorable region to observe shadow states in ARPES is near $(\pi/2, \pi/2)$, where the main and shadow band are well separated. Near $(\pi, 0)$ the absolute intensity of the shadow states is largest, but they are difficult to detect because of their superposition with the dominant main band.

The superconducting state of the bilayer Hubbard model was treated by using a strong coupling Eliashberg theory within the FLEX approximation.²³ By assuming that there is no interband pairing,²⁵ one obtains one order parameter for each band, namely $\phi_{\pm}(\mathbf{k}, \omega)$. These are connected to the layer representation via $\phi_{\pm}(\mathbf{k}, \omega) = \phi_{\parallel}(\mathbf{k}, \omega) \pm \phi_{\perp}(\mathbf{k}, \omega)$, where $\phi_{\parallel}(\mathbf{k}, \omega)$ ($\phi_{\perp}(\mathbf{k}, \omega)$) describes intra- (inter-) layer Cooper pair formation. By solving these equations for the YBCO dispersion with $t_{\perp}=0$, we find for all x a $d_{x^2-y^2}$ -wave superconducting state ($T_c=70$ K for $x=0.08$). Concerning the pairing symmetry in a bilayer system and in view of our results for the effective interactions, the argumentation of Ref. 12 might apply to low doping and might cause a change from d - to s -wave pairing. To clarify this important point, we present in Fig. 4 our results for T well below T_c and the YBCO-like model with $t_{\perp}=0.4t$ and $x=0.08$ in comparison with $t_{\perp}=0$. Here in contrast to the single layer case, where only a d -wave pairing state occurs [Fig. 4(a)], we find an s^{\pm} state as a solution of the Eliashberg equations as shown in Fig. 4(b). Nevertheless, the s^{\pm} state refers only to a metastable solution, since the bilayer $d_{x^2-y^2}$ pairing symmetry, as shown in Figs. 4(c) and 4(d), still yields $\phi^d \gg \phi^s$ and consequently a much larger condensation energy ($T_c=75$ K for $x=0.08$). Interestingly, the d -wave state is characterized by an increasing contribution of interlayer pairing with decreasing doping, where for $x=0.08$ Cooper pairs are formed by electrons from the same layer as from different layers with almost equal probability.

One of the most characteristic properties of the cuprates is the occurrence of an *optimal doping*. To investigate the influence of the bilayer coupling on the superconducting phase transition we use the LSCO-like dispersion for comparison with previous results where the *optimal doping* was found to be at $x=0.13$.²⁴ We calculated T_c from the condition

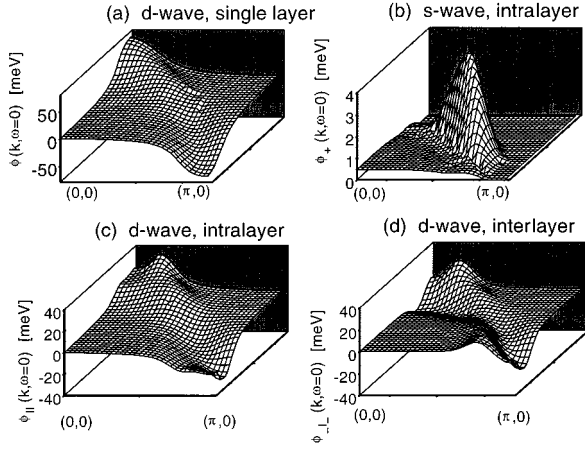


FIG. 4. Superconducting order parameter for $T=48$ K, $U=4t$, and the YBCO dispersion. (a) single layer ($t_{\perp}=0$, $T_c=70$ K). (b) metastable bilayer s^{\pm} state for the antibonding band. (c and d) bilayer d -wave state in the layer representation ($t_{\perp}=0.4t$, $T_c=75$ K).

$\Delta_0=0$ with $\Delta_0=\text{Re}\Delta(\mathbf{k},\Delta_0)$ to account for the fluctuation effects of the superconducting state.²⁴ Here we find that T_c is suppressed for small doping ($x=0.09$: $T_c^{\text{mono}}=85$ K to $T_c^{\text{bi}}=77$ K) with respect to the monolayer whereas it is enhanced for larger x ($x=0.16$: $T_c^{\text{mono}}=95$ K to $T_c^{\text{bi}}=107$ K). Thus, the *optimal doping* is shifted to larger x which is in

correspondence to our prediction that shadow states are only observable below this critical doping concentration.²⁴ Furthermore this remarkable behavior is directly related to the $d_{x^2-y^2}$ symmetry of superconductivity. Although the bilayer pairing state yields a significant interlayer contribution, the additional energy gain compared to the monolayer has to compete with the loss caused by magnetic frustration. Here the bilayer coupling interferes with the interplane d -wave superconductivity since two ferromagnetically oriented spins would be coupled in the case of a perfect antiferromagnet which can only be allowed due to the dynamical short range order. Therefore, the dependence of T_c on t_{\perp} for a given doping concentration depends sensitively on which contribution is dominant. For larger doping, the magnetic correlation length ξ is relatively small ($\sim 2-3$ lattice spacings)²¹ and thus T_c increases due to the interlayer Cooper pairing, whereas for small doping, the region of tightly arranged antiferromagnetically correlated spins is much larger leading to a lower T_c .²⁶

In conclusion, we presented new results for the bilayer Hubbard model by using the FLEX approximation. The antiferromagnetic coupling between the layers leads to an enhanced shadow state intensity and to their observability in YBCO- and BSCCO-like models. We found that the bilayer splitting is reduced ($\sim 50\%$) and the interlayer hopping is effectively blocked for small doping. Finally, the superconducting d -wave order parameter has significant interlayer contributions causing the *optimal doping* to shift further away from half filling.

¹J.M. Tranquada *et al.*, Phys. Rev. B **46**, 5561 (1992).
²R. Liu *et al.*, Phys. Rev. B **46**, 11 056 (1992).
³H. Ding *et al.*, Phys. Rev. Lett. **76**, 1533 (1996).
⁴Z.X. Shen and D.S. Dessau, Phys. Rep. **253**, 1 (1995).
⁵N.E. Bickers *et al.*, Phys. Rev. Lett. **62**, 961 (1989).
⁶P. Aebi *et al.*, Phys. Rev. Lett. **72**, 2757 (1994).
⁷A. Milis *et al.*, Phys. Rev. Lett. **70**, 2810 (1993).
⁸N. Bulut *et al.*, Phys. Rev. B **45**, 5577 (1992).
⁹R.T. Scalettar *et al.*, Phys. Rev. B **50**, 13 419 (1994).
¹⁰A.I. Lichtenstein *et al.* (unpublished).
¹¹T. Dahm and L. Tewordt, Physica C **253**, 334 (1995).
¹²A.I. Lichtenstein *et al.*, Phys. Rev. Lett. **74**, 2303 (1995).
¹³J. Schmalian, M. Langer, S. Grabowski, and K.H. Bennemann, Comput. Phys. Commun. **93**, 141 (1996).
¹⁴This dispersion is used, since its FS is closed around (π, π) . These parameters lead for $U > 2.5t$ and $t_{\perp} = 0 - 0.8t$ to commensurate peaks in $V_{\parallel}(\mathbf{k}, \omega)$ as observed in experiments 1.
¹⁵O.K. Andersen *et al.*, J. Phys. Chem. Solids **56**, 1573 (1995).
¹⁶R.H. Howell *et al.*, Phys. Rev. B **49**, 13 127 (1994).
¹⁷For YBCO and $x=0.12$ we find $\Delta\varepsilon(\mathbf{k}=(\pi,0)) \approx 80$ meV that is comparable with experimental indications of $\Delta\varepsilon^{\text{exp}}(\mathbf{k}=(\pi,0)) \approx 110$ meV 2.
¹⁸S. Chakravarty *et al.*, Science **261**, 337 (1993).
¹⁹S.L. Cooper and K.E. Gray, in *Physical Properties of High- T_c Superconductors IV*, edited by D.M. Ginsberg (World Scientific, Singapore, 1994).

²⁰R.J. Radtke *et al.*, Phys. Rev. B **53**, R552 (1996).
²¹M. Langer, J. Schmalian, S. Grabowski, and K.H. Bennemann, Phys. Rev. Lett. **75**, 4508 (1995).
²²Due to the similarity of the BSCCO and YBCO FS's, we used the bare intraplane dispersion of YBCO and $t_{\perp}(\mathbf{k}) = 1/4t_{\perp}[\cos(k_x) - \cos(k_y)]^2$ with $t_{\perp} = 0.4t$. The resulting FS is similar to the experiments 4 and a similar shadow band formation as in our YBCO model occurs.
²³The Eliashberg equations for our bilayer model are similar to the single layer case 24 when a third dimension with two momenta is introduced.
²⁴S. Grabowski, M. Langer, J. Schmalian, and K.H. Bennemann, Europhys. Lett. **34**, 219 (1996).
²⁵Due to the bilayer inversion symmetry the equations for even- and the odd-parity pairing decouple where the first one yields $\phi_{\perp}(\mathbf{k}, \omega) \neq 0$ and a larger T_c than the odd (interband) pairing state with $\phi_{\perp}(\mathbf{k}, \omega) = 0$. See also J. Maly *et al.*, Phys. Rev. B **53**, 6786 (1996).
²⁶These results seem to be in contrast to recent QMC studies of Ref. 9, where the particle-particle vertex decreases with t_{\perp} . This can be understood since these simulations were performed at large T ($T \approx 5T_c$) where the increased bandwidth of the bilayer should dominate the pairing correlations. However, for low- T our results show that the pairing interaction is primarily influenced by the additional interlayer spin dynamics.